Electrospinning of Porous Silica Nanofibers Containing Silver Nanoparticles for Catalytic Applications

Alpa C. Patel,[†] Shuxi Li,[†] Ce Wang,[‡] Wanjin Zhang,[‡] and Yen Wei*[,†,‡]

Department of Chemistry, Drexel University, Philadelphia, Pennsylvania 19104, and The Alan G. MacDiarmid Institute, Jilin University, Changchun 130012, China

Received June 7, 2006. Revised Manuscript Received January 8, 2007

Porous silica nanofibers containing catalytic silver nanoparticles have been synthesized by a new method that combines sol−gel chemistry and electrospinning technique. Tetraethyl orthosilicate (TEOS), poly-[3-(trimethoxysily)propyl methacrylate] (PMCM), and silver nitrate ($AgNO_3$) were used as precursors for the production of silica−PMCM hybrid fibers containing $AgNO_3$. Calcination of the hybrid fibers at high temperatures results in porous silica fibers because of thermal decomposition of PMCM polymer and in conversion of $AgNO_3$ to silver nanoparticles. The color of the fiber mats changed from white to dark golden yellow due to the surface plasma resonance of the silver nanoparticles embedded in the fibers. The size and density of the silver particles in the silica fibers could be tuned by varying the size of the fibers, amount of $AgNO_3$ introduced, and the thermal treatment conditions. The silica fibers containing silver particles were characterized with environmental scanning electron microscopy, transmission electron microscopy, X-ray diffraction, UV−vis spectroscopy, and thermogravimetric analysis. The catalytic activity of the silver containing fiber mats was assessed by a reduction reaction of methylene blue dye.

Introduction

During the past decade, metal nanoparticles have found a niche in various fields of science, ranging from chemistry to physics, and to biotechnology.[1,2] Because of their nanoscale, optical,[3] electrical,[4] and catalytic properties,[3,5,6] metal nanoparticles have been exploited for unique applications as sensors,[7] optical switches,[8] biological markers,[9] nanoelectronic devices,[10] and catalysts[11] for many chemical and biological reactions. Among the important chemical reactions for which they exclusively demonstrate to have high catalytic activity are hydrogenation, hydroformylation, carbonylation, and so forth.[12−15] However, due to the easy aggregation, deactivation, and poisoning, the metal nanoparticles have proven undesirable for large scale use.[16] Thus, research efforts have been made to protect the particles by stabilization in colloidal solutions containing surfactants and by formation of complexes with polymer ligands.[17,18] Though the particles have been stabilized successfully using these techniques, they would not be reused as catalysts. The stabilization process could also cause loss in activity of the particles and, hence, render the catalysts more expensive. Therefore, to utilize metal nanoparticles for various catalytic applications in the most efficient way, it is necessary to explore novel techniques for metal particle stabilization.

The nanoscale dispersion of metal nanoparticles in polymers,[19,20] silicates,[21] and metal oxide[22] substrates, on the other hand, have attracted great interest because of their stability, reusability, and good catalytic properties.[23−25] Various metals

* Corresponding author. Phone: (215)895-2650. Fax (215)895-1265. E-mail: weiyen@drexel.edu.
[†] Drexel University.
[‡] Jilin University.

(1) Henglein, A. *Chem. Mater.* **1998**, *10* (1), 444−450.
(2) Mostafavi, M.; Marignier, J. L.; Amblard, J.; Belloni, J. *Radiat. Phys. Chem.* **1989**, *34* (4), 605−617.
(3) Moller, K.; Bein, T. *Chem. Mater.* **1998**, *10* (10), 2950−2963.
(4) Anderson, M. L.; Morris, C. A.; Stroud, R. M.; Merzbacher, C. I.; Rolison, D. R. *Langmuir* **1999**, *15* (3), 674−681.
(5) Morey, M. S.; Bryan, J. D.; Schwarz, S.; Stucky, G. D. *Chem. Mater.* **2000**, *12* (11), 3435−3444.
(6) Ying, J. Y.; Mehnert, C. P.; Wong, M. S. *Angew. Chem., Int. Ed.* **1999**, *38* (1/2), 56−77.
(7) Whetten, R. L.; Shafigullin, M. N.; Khoury, J. T.; Schaaff, T. G.; Vezmar, I.; Alvarez, M. M.; Wilkinson, A. *Acc. Chem. Res.* **1999**, *32* (5), 397−406.
(8) Francois, L.; Mostafavi, M.; Belloni, J.; Delouis, J. F.; Delaire, J.; Feneyrou, P. *J. Phys. Chem. B* **2000**, *104* (26), 6133−6137.
(9) Glynou, K.; Ioannou, P. C.; Christopoulos, T. K.; Syriopoulou, V. *Anal. Chem.* **2003**, *75* (16), 4155−4160.
(10) Greenwood, N. N.; Earnshaw, A. *Chemistry of the Elements*, 2nd ed.; Butterworth-Heinemann: Oxford, 1997.
(11) Mehnert, C. P.; Weaver, D. W.; Ying, J. Y. *J. Am. Chem. Soc.* **1998**, *120* (47), 12289−12296.
(12) Pradhan, N.; Pal, A.; Pal, T. *Colloids Surf., A* **2002**, *196* (2−3), 247−257.
(13) Zaera, F.; Gellman, A. J.; Somorjai, G. A. *Acc. Chem. Res.* **1986**, *19* (1), 24−31.
(14) Fendler, J. H. *Chem. Rev.* **1987**, *87* (5), 877−899.
(15) Hercules, D. M.; Proctor, A.; Houalla, M. *Acc. Chem. Res.* **1994**, *27* (12), 387−393.
(16) Canamares, M. V.; Garcia-Ramos, J. V.; Gomez-Varga, J. D.; Domingo, C.; Sanchez-Cortes, S. *Langmuir* **2005**, *21* (18), 8546−8553.
(17) Schmid, G. *Chem. Rev.* **1992**, *92* (8), 1709−1727.
(18) Lewis, L. N. *Chem. Rev.* **1993**, *93* (8), 2693−2730.
(19) Zheng, M.; Gu, M.; Jin, Y.; Jin, G. *Mater. Res. Bull.* **2001**, *36*, 853−859.
(20) Li, L.; Cao, X.; Yu, F.; Yao, Z.; Xie, Y. *J. Colloid Interface Sci.* **2003**, *261* (2), 366−371.
(21) Chakrabarti, K.; Whang, C. M. *Mater. Sci. Eng., B* **2002**, *B88* (1), 26−34.
(22) Epifani, M.; Giannini, C.; Tapfer, L.; Vasanelli, L. *J. Am. Ceram. Soc.* **2000**, *83* (10), 2385−2393.
(23) Pal, T.; De, S.; Jana, N. R.; Pradhan, N.; Mandal, R.; Pal, A.; Beezer, A. E.; Mitchell, J. C. *Langmuir* **1998**, *14* (17), 4724−4730.
(24) Kundu, S.; Mandal, M.; Ghosh, S. K.; Pal, T. *J. Colloid Interface Sci.* **2004**, *272* (1), 134−144.

10.1021/cm061331z CCC: $37.00
Published on Web 02/23/2007

like gold, platinum, palladium, silver, and so forth[11,22] have been encapsulated using methods like chemical vapor deposition,[11] and reduction of metal salts by thermal,[26] chemical,[27] or UV light[1] treatment. For metal nanocomposites to perform as good catalysts, they should possess three important characteristics: (1) the substrate should have high surface area,[6,28,29] (2) the nanoparticles present inside the substrate should be easily accessible to various chemical reagents,[28] and (3) the size and distribution of the nanoparticles in the substrate should be uniform.[22] The substrates used for metal particle encapsulation include metal oxides,[22,29] organically modified silicates,[21] polymers shaped as thin films,[19,30] spheres,[31,32] fibers,[27,33] dendrimers,[20] and so forth. Among these substrates, fibrous materials show unique properties suitable for use as catalysts. Some of the main benefits of fibrous catalysts include flexibility of form, low resistance to flow of gas and liquids through a bundle of fibers, high surface area, safer operations, easy scale up, and reusability.[34] Some specific examples of fibrous material include metal wires in the form of gauzes,[35] fiberglass materials,[36] and carbon fibers.[37] These materials act as excellent carriers for supporting catalytic particles.

Electrospining is a widely employed method in recent years to produce polymer nanofiber mats with high surface area, which could be used as metal supporting substrates for catalytic applications.[27,38−42] Some of the obstacles scientists have to overcome in order to utilize this technique for metal nanoparticle encapsulation and for catalytic applications include aggregation of nanoparticles, poisoning of surface stabilized particles, and limited resistance of the polymer fibers to strong organic solvents and high temperature.

To address the above-mentioned problems, we have developed a facile method that combines sol−gel processing with electrospinning technique to prepare porous silica nanofibers containing uniformly distributed silver nanoparticles (PSFSP). The unique features, which make PSFSP ideal candidate for catalytic applications could include (1) high sensitivity and reactivity of porous silica nanofibers because of large surface area (average fiber diameter of 100 nm, fiber length of up to 10 cm and surface area of 600 $m^2\ g^{-1}$), (2) resistance to high temperature and strong solvents making the catalytic fibers usable and reusable under harsh conditions, (3) easy control of size and density of metal nanoparticles in the fibers, and finally (4) the freedom to encapsulate various kinds of nanoparticles including gold, palladium, quantum dots, and so forth.

Tetraethylorthosilicate (TEOS), trimethoxysilyl functionalized polymethacrylate copolymer (PMCM), and silver nitrate ($AgNO_3$) are the main precursors used to synthesize PSFSP. It has been well established in our laboratory that the sol−gel reactions between the inorganic precursor TEOS and the polymer precursor PMCM could afford organic vinyl polymer−inorganic silica hybrid materials, in which the polymer chains are uniformly distributed in and covalently bonded to silica network.[43−45] In this work, the polymer−silica hybrid materials are employed to disperse silver nitrate and to be electrospun into nanofibers. The electrospun fibers were heat treated to produce silver nanoparticles via $AgNO_3$ reduction and to pyrolyze the polymethacrylate component rendering the final silica fibers porous. Various electron microscopic and spectroscopic characterizations were performed to study the effects of concentration of $AgNO_3$ and PMCM on the morphology of the silica fiber and the effect of heat treatment on the production of silver nanoparticles. The catalytic efficiency of the silver nanoparticles encapsulated inside porous silica fibers was evaluated in a silver catalyzed reduction of methylene blue dye (MB) by sodium borohydride ($NaBH_4$) under nitrogen. The reaction is thermodynamically favorable, and the color change from a blue in its oxidized state to colorless in its reduced state can be easily detected using a simple UV−vis spectroscopy method.[46,47]

Experimental Section

Materials and Reagents. Tetraethylorthosilicate (TEOS, 98%), silver nitrate ($AgNO_3$, 2 N solution in water), nitric acid (HNO_3, 1 N solution in water), reagent grade tetrahydrofuran (THF, 99.9%), and sodium borohydride ($NaBH_4$, 99.9%) were all purchased from Sigma-Aldrich Chemical Co. and used as received. Trimethoxysilyl functionalized methacrylate copolymer (PMCM, M_n 58000, see Supporting Information for chemical structure, Scheme S1) was synthesized by free radical copolymerization of trimethoxysilylpropyl methacrylate with methyl methacrylate in a 1:9 molar ratio, following the previously reported procedures by Wei et al.[48,49]

Preparation of Spinning Solution. Scheme 1 shows briefly the important steps involved in the fabrication of PSFSP. The first step

(25) Pradhan, N.; Pal, A.; Pal, T. *Colloids Surf., A* **2002**, *196* (2−3), 247−257.
(26) Shi, H.; Zhang, L.; Cai, W. *J. Appl. Phys.* **2000**, *87* (3), 1572−1574.
(27) Demir, M. M.; Gulgun, M. A.; Menceloglu, Y. Z.; Erman, B.; Abramchuk, S. S.; Makhaeva, E. E.; Khokhlov, A. R.; Matveeva, V. G.; Sulman, M. G. *Macromolecules* **2004**, *37* (5), 1787−1792.
(28) Bronstein, L. M.; Polarz, S.; Smarsly, B.; Antonietti, M. *Adv. Mater.* **2001**, *13* (17), 1333−1336.
(29) Khushalani, D.; Hasenzahl, S.; Mann, S. *J. Nanosci. Nanotechnol.* **2001**, *1* (2), 129−132.
(30) Bharathi, S.; Nogami, M.; Ikeda, S. *Langmuir* **2001**, *17* (24), 7468−7471.
(31) Jiang, T.; Chen, W.; Zhao, F.; Liu, Y.; Wang, R.; Du, H.; Zhang, T. *J. Appl. Polym. Sci.* **2005**, *98* (3), 1296−1299.
(32) Lin, K. J.; Chen, L. J.; Prasad, M. R.; Cheng, C. Y. *Adv. Mater.* **2004**, *16* (20), 1845−1849.
(33) Huang, Z. M.; Zhang, Y. Z.; Kotaki, M.; Ramakrishna, S. *Compos. Sci. Technol.* **2003**, *63* (15), 2223−2253.
(34) Matatov-Meytal, Y.; Sheintuch, M. *Appl. Catal., A* **2002**, *231* (1−2), 1−16.
(35) Horner, B. T. *Platinum Met. Rev.* **1993**, *37* (2), 76−85.
(36) Neyestanaki, A. K.; Lindfors, L. E. *Combust. Sci. Technol.* **1994**, *97* (1−3.), 121−136.
(37) Serp, P.; Corrias, M.; Kalck, P. *Appl. Catal., A* **2003**, *253* (2), 337−358.
(38) An, L.; Wang, Y. *Dangdai Shiyou Shihua* **2002**, *10* (1), 41−45.
(39) Dai, L. *Encycl. Nanosci. Nanotechnol.* **2004**, *8*, 763−790.
(40) Ramakrishna, S. *An Introduction to Electrospinning and Nanofibers*; World Scientific Publishing Company: River Edge, NJ, 2005.
(41) Wang, C.; Li, Z. Y.; Li, D.; Yang, Q. B.; Hong, Y. *Int. J. Nanosci.* **2002**, *1* (5 and 6), 471−476.
(42) Yang, Q. B.; Li, D. M.; Hong, Y. L.; Li, Z. Y.; Wang, C.; Qiu, S. L.; Wei, Y. *Synth. Met.* **2003**, *137* (1−3.), 973−974.
(43) Wei, Y.; Bakthavatchalam, R.; Whitecar, C. K. *Chem. Mater.* **1990**, *2* (4), 337−339.
(44) Wei, Y.; Yang, D.; Bakthavatchalam, R. *Mater. Lett.* **1992**, *13* (4−5), 261−266.
(45) Wei, Y.; Wang, W.; Yang, D.; Tang, L. *Chem. Mater.* **1994**, *6* (10), 1737−1741.
(46) Jana, N. R.; Sau, T. K.; Pal, T. *J. Phys. Chem. B* **1999**, *103* (1), 115−121.
(47) Jiang, Z. J.; Liu, C. Y.; Sun, L. W. *J. Phys. Chem. B* **2005**, *109* (5), 1730−1735.
(48) Wei, Y.; Jin, D.; Yang, C.; Kels, M. C.; Qiu, K. Y. *Mater. Sci. Eng. C* **1998**, *C6* (2, 3), 91−98.

Scheme 1. Experimental Flow Chart for Synthesis of Porous Silica Nanofibers Containing Silver Nanoparticles

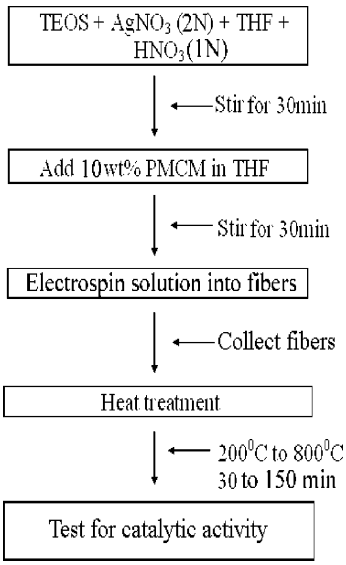

was to generate the silicate/$AgNO_3$ sol preparation. Thus, TEOS was mixed with THF, and then, a mixture of 2 N $AgNO_3$ and 1 N HNO_3 was added dropwise at two different [TEOS]/[THF]: [HNO_3, 1 N]/[$AgNO_3$, 2 N] molar ratios of 1:2:0.05:0.06 and 1:2:0.05:0.1 with constant stirring for 30 min at room temperature. The water required for hydrolysis of TEOS was obtained from the dilute $AgNO_3$ solution used in the preparation of the sol. Next, 10 wt % PMCM solution in THF was added dropwise to the hydrolyzed TEOS/$AgNO_3$ sol with constant stirring to obtain a transparent homogeneous solution with a viscosity of around 60−70 cP and a final PMCM content of 2−4 wt %, with respect to the wt % of silica.

Electrospinning. The spinning solution thus prepared was collected in a pipet with a tip opening of approximately 0.5 mm. An electric field of 20 kV (Gamma High Voltage Research D-ES30) was then applied by dipping a charged copper wire directly into the spinning solution. A grounded aluminum plate placed at a distance of 20 cm from the tip of the pipet was used as a fiber collecting device. Under the electric field, a droplet suspended from the tip of the pipet acted as the feed source from which a charged jet of hydrolyzed TEOS/$AgNO_3$/PMCM sol solution was ejected out in the form of nanofibers. The two sets of PMCM modified fibers containing 0.06 and 0.1 mol $AgNO_3$ with respect to 1 mol TEOS thus collected were then subjected to varying heat treatments, which caused the hydrolyzed TEOS to reduce to silica, the PMCM polymer to degrade, and the $AgNO_3$ salt present in the fibers to reduce to silver nanoparticles, finally producing porous silica fibers containing approximately 10 and 20 wt % silver nanoparticles, respectively.

Catalysis. The catalytic activity of the silver nanoparticles in the fibers was analyzed following the literature procedure.[23,50] For a typical procedure, a certain amount of silica fibers containing 10 wt % silver nanoparticles was homogeneously dispersed into a MB dye solution in water (2 mL, 0.01 mol/L), followed by injecting aqueous $NaBH_4$ (1 mL, 0.1 mol/L) rapidly under constant stirring. The blue color of the mixture gradually vanished, indicating the silver catalyzed reduction of the dye. The rate of color disappearance, as indicative of catalytic activity of silver particles, was monitored with UV−vis spectrometer.

(49) Wei, Y.; Feng, Q.; Xu, J.; Dong, H.; Qiu, K. Y.; Jansen, S. A.; Yin, R.; Ong, K. K. *Adv. Mater.* **2000**, *12* (19), 1448−1450.
(50) Jana, N. R.; Pal, T. *Langmuir* **1999**, *15* (10), 3458−3463.

Table 1. Sample Code and Average Diameter of Silica Fibers and Silver Nanoparticles Subjected to Various Heat Treatments

		av diameter SF10[a]			av diameter SF20[a]		
			Ag nanoparticles, nm			Ag nanoparticles, nm	
T,[b] °C	*t*,[b] min	silica fibers,[c] nm	TEM[d]	XRD[e]	silica fibers,[c] 5nm	TEM[d]	XRD[e]
30		180 ± 10			290 ± 10		
200	30	175 ± 15			290 ± 30		
	60	174 ± 17			280 ± 10		
	150	170 ± 17			280 ± 20		
400	30	150 ± 20			265 ± 10		
	60	150 ± 12	10	8.5	258 ± 17	12	11
	150	135 ± 15	13	11	250 ± 15	16	14.5
600	30	130 ± 17	13	11	252 ± 10	15	14
	60	100 ± 17	16	14	252 ± 30	22	18.5
	150	100 ± 20	20	19	248 ± 25	25	21

[a] Average diameter of heat-treated silica nanofibers SF10 and SF20 containing 10 wt % silver nanoparticles and 20 wt % silver nanoparticles, respectively. [b] Various temperature and times used to heat treat PMCM modified electrospun silica fibers. [c] Average diameter (mean ± standard deviation) of SF10 and SF20 obtained by measuring 100 fibers of a single sample from ESEM micrographs after heat treatment. [d] Average diameter of silver nanoparticles present in SF10 and SF20 obtained by measuring 40 nanoparticles from TEM micrographs. [e] Diameter of silver nanoparticles in SF10 and SF20 obtained from the Bragg's and Sherrer's equation calculated using the XRD graph.

Instrumentation. Gel permeation chromatography (GPC, Hewlett-Packard HP 1090), equipped with a refractive index detector and a PLgel column, was used to determine the molecular weight of the PMCM copolymer. A digital viscometer (Brookfield instruments, model DV-II+) was used to determine the viscosity of the spinning solution, and infrared spectra (FT-IR, Perkin-Elmer 1600 spectrophotometer, 4 cm^{-1} resolution, 200 scans) of the fiber samples were measured in the form of KBr powder-pressed pellets under ambient conditions. Field emission environmental scanning electron microscope (ESEM, Phillips XL-30) operated at an accelerating voltage of 15 kV, and equipped with an energy dispersive X-ray analyzer (EDX), was used to measure the diameter of fibers and elemental analysis, respectively. A transmission electron microscope (TEM, JEOL 2000FX), operated at the accelerating voltage of 300 kV, was used to study the internal morphology of the PSFSP. The samples for TEM micrographs were prepared by embedding the fibers into a resin and microtoming the resin into 100 nm thick cross sections. A thermogravimetric analyzer (TGA, TA Q50, 40−700 °C at 10 °C/min, in air) was used to heat the electrospun silica fibers for the degradation of PMCM polymer and formation of silver nanoparticles. The before and after heat-treated fibers were analyzed for surface area using the N_2 sorption characterization method (Micromeritics ASAP 2010). Heat-treated fiber square mats (2 × 2 cm^2) were used to study the optical properties of the fibers using large angle X-ray diffraction [XRD, Siemens D-500, Cu Kα radiation ($\lambda = 1.542$ Å) using 1.35 KW Cu X-ray tube] and solid-state UV−vis reflectance spectrophotometer (UV−Vis, Perkin-Elmer-330, 200−800 cm^{-1} wavelength).

Results and Discussion

All the fibers studied and analyzed were synthesized using similar electrospinning parameters as stated in the Experimental Section (i.e., pipet tip diameter of 0.5 mm, voltage of 20 kV, fiber collecting distance of 20 cm). Approximately 10 ESEM micrographs were taken randomly from different regions of a 20 × 20 cm^2 square silica fiber mat, and the average fiber diameter (Table 1) of 100 silica fibers from each sample was then measured using UTHSCSA ImageTool 3.0.

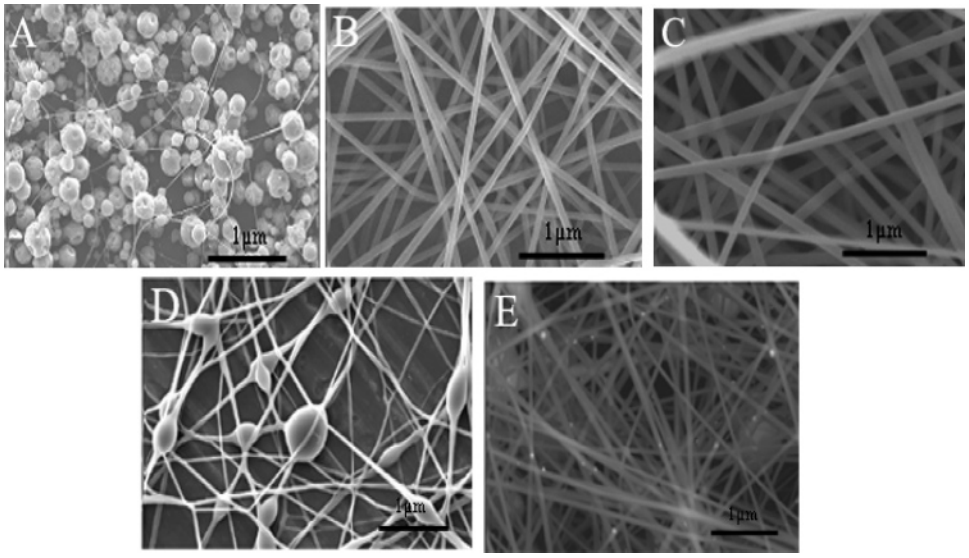

Figure 1. ESEM images of non-heat-treated electrospun silica/$AgNO_3$ nanofibers containing (A) 0 wt % PMCM and 0.06 mol $AgNO_3$, (B) 2 wt % PMCM and 0.06 mol $AgNO_3$, (C) 6 wt % PMCM and 0.06 mol $AgNO_3$, and (D) 2 wt % PMCM and 0.1 mol $AgNO_3$. (E) ESEM images of heat-treated silica fibers (600 °C for 60 min) which were electrospun with a solution containing 2 wt % PMCM and 0.06 mol $AgNO_3$. Scale bar: 5 μm.

Figure 1A,B,C shows fibers containing, respectively, 0, 2, and 6 wt % of PMCM polymer with respect to the weight of silica. Silica fibers spun without any PMCM showed beaded morphology due to the low molecular weight and low viscosity of the sol−gel silicates in the spinning solution (10 cP). On the other hand, the long molecular chains of the PMCM copolymer when added to the spinning solution tend to get entangled with the smaller silica sol molecules forming covalent bonds via the cross-condensation of the silanol groups (i.e., Si−OH) in both TEOS and PMCM.[49] Silica fibers spun with 2 wt % PMCM show a uniform morphology with average diameter of around 180 ± 10 nm (Table 1). As the wt % of PMCM is increased from 2 to 6 wt %, the viscosity of the spinning solution also increases from 40 to 60 cP, which in turn increases the diameter of the fibers from 180 ± 10 nm to 290 ± 10 nm. The increase in diameter of fibers with viscosity has been noticed previously in many electrospun polymer fibers.[40] Hence, all silica fibers studied from here on contain 2 wt % of PMCM (with respect to silica), unless otherwise stated. The amount of $AgNO_3$ added to the spinning silica solution also plays a role in governing the morphology of the fibers. Increasing the amount of $AgNO_3$ from 0.06 mol (10 wt % silver) to 0.1 mol (20 wt % silver) in the spinning solution caused the fibers to stick together as well as an increase in the diameter of the spun fibers (Table 1, Figure 1B,D). This surface morphology change could be attributed to the localized charge effects on the surface of the fibers, as well as slow evaporation of water from the fibers, causing the wet fibers to stick together during electrospinning.[27,33,51] All silica fibers discussed from here on contain 10 wt % silver (0.06 mol $AgNO_3$) with respect to silica, unless otherwise stated. Thus, a narrow size distribution of the diameter of the silica fibers, with smooth morphology, can be obtained by regulating the amount of PMCM and $AgNO_3$ added into the spinning solution.

The electrospun fibers were then heated in air, to various temperatures and time (Table 1), at the rate of 10 °C/min, using a thermogravimetric analyzer (TGA). These fibers were then analyzed for surface area and porosity (Micromeritics ASAP 2010). As anticipated, degradation of PMCM polymer inside the fibers during heat treatment led to the increases in surface area from 11 $m^2\ g^{-1}$ for non-heat-treated fibers to 600 $m^2\ g^{-1}$ for heat-treated fibers. The TEM micrograph images (Figure 2) of the heat-treated silica fibers clearly show a homogeneous distribution of silver nanoparticles inside the porous silica fibers. The wt % of silver in the heat-treated silica fibers which were experimentally determined via the EDX and X-ray mapping technique (Supporting Information, Figures S1 and S2) was found to be around 9 wt %, which is close to the actual stoichiometric value of silver (10 wt %), calculated from the electrospinning hydrolyzed TEOS/(0.06 mol)$AgNO_3$ solution mixture. The chemical and morphological changes that take place during heat treatment of electrospun fibers can be evaluated by studying the FT-IR and TGA data for electrospun silica fibers before and after heat treatment. Figure 3 represents characteristic FT-IR absorption bands at 1730 cm^{-1} (C═O) for pure PMCM polymer, at 900 cm^{-1}, 3500 cm^{-1} (Si−OH) for PMCM modified silica fibers before heat treatment, and at 1081 cm^{-1} (Si−O−Si) for heat-treated silica fibers. As the temperature of the fibers was increased from 200 to 600 °C, a gradual decrease in the Si−OH band and an increase in the Si−O−Si band were observed due to the complete condensation of hydrolyzed silica precursor (Si−OH) to silica (SiO_2).[48] As the electrospun silica fibers have only a small amount of PMCM polymer (2 wt %), the characteristic (C═O) peak for PMCM in the silica fibers is not clearly visible.[52,53] Figure 4 shows TGA and its first derivative curves for pure PMCM polymer, pure silica, and electrospun silica/$AgNO_3$ fibers

(51) Dai, H.; Gong, J.; Kim, H.; Lee, D. *Nanotechnology* **2002**, *13* (5), 674−677.

(52) Desai, K.; Sung, C. *Mater. Res. Soc. Symp. Proc.* **2002**, *736*, 121−126.

(53) Chan, C. K.; Peng, S. L.; Chu, I. M.; Ni, S. C. *Polymer* **2001**, *42* (9), 4189−4196.

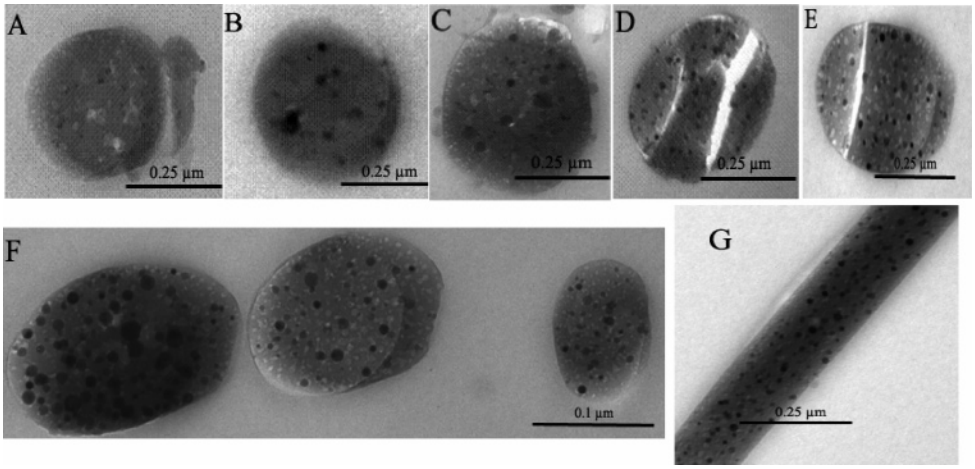

Figure 2. TEM cross section micrographs of electrospun porous (light features: pores) silica containing silver nanoparticles (dark spherical regions) after thermal treatment (wt % of silver, time of heat treatment, temperature of heat treatment): (A) 10 wt %, 60 min, 400 °C; (B) 10 wt %, 60 min, 600 °C; (C) 10 wt %, 60 min, 800 °C; (D) 10 wt %, 150 min, 400 °C; (E) 20 wt %, 60 min, 400 °C; (F) 10 wt %, 150 min, 600 °C (showing fiber diameters from 100 to 250 nm). (G) TEM cross section micrograph of a silica fiber showing homogeneous distribution of silver nanoparticles along the fiber, too. Scale bar: 250 nm.

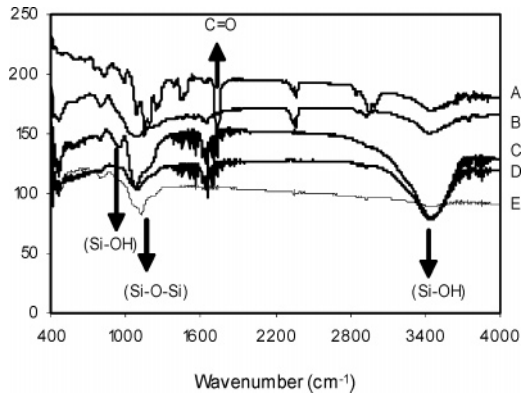

Figure 3. Infrared spectra of (A) pure PMCM polymer, (B) pure silica, (C) hydrolyzed TEOS/$AgNO_3$/2 wt % PMCM electrospun fibers before heat treatment, (D) silica fibers containing 10 wt % silver nanoparticles heated at 200 °C for 30 min, and (E) silica fibers containing 10 wt % silver nanoparticles heated at 600 °C for 30 min. (The *y*-axis is transmittance with relatively labeled values because of superposition of spectra.)

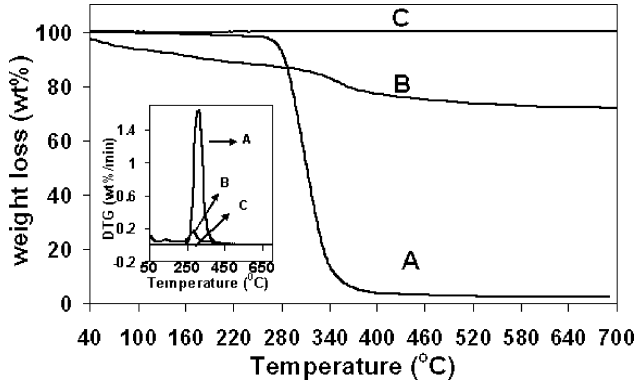

Figure 4. Thermogravimetric analysis (TGA) and deconvoluted derivative thermogravimetric (DTG) curves for samples heated at 10 °C/min from 40 to 800 °C in air: (A) pure PMCM polymer, (B) PMCM modified silica fibers containing 0.06 mol $AgNO_3$ before heat treatment, and (C) pure SiO_2.

containing 2 wt % PMCM. Pure silica does not show any degradation due to its high temperature stability. A degradation maximum for both pure PMCM and silica fibers containing 2 wt % PMCM at around 300 °C is noticed. As the temperature is increased further, the pure PMCM polymer degrades completely leaving behind only minute amounts of silica (SiO_2).[48] On the other hand, the complete decomposition of 2 wt % of PMCM present in the silica fibers makes the fibers porous (Figure 2) and, hence, increases the surface area and catalytic efficiency of the fibers. At the same time, as the electrospun silica/$AgNO_3$ fibers are heated to temperatures above 300 °C, the $AgNO_3$ salt present in the fibers is reduced to evenly distribute silver nanoparticles (Figure 2).[22] The high-temperature treatment would also drive remaining silica precursor (hydrolyzed TEOS) in the fibers to further condense to SiO_2[6,53] with the release of small molecule byproducts such as ethanol and water from the fibers, which resulted in the fibers shrinking a little (Table 1, Figure 1B,E), yet maintaining high porosity. Unlike organic polymers, which show major shrinkage and degradation at high temperatures,[54] the rigid network of inorganic silica enables the silica fibers to retain their shape, prevents major shrinkage, and makes the fibers resistant to organic chemicals.

In order to optimize the catalytic efficiency of the silver nanoparticles present in the porous silica fibers, a controlled and reproducible size distribution along with high density of silver nanoparticles has to be achieved. Thus, the factors affecting the size of the silver nanoparticles must be evaluated. Table 1 lists the size of the silver nanoparticles which were obtained by measuring 40 silver nanoparticles form each sample via the TEM micrographs (Figure 2). The size of the silver nanoparticles present in the heat-treated silica fibers (Figure 2A−C, 250 nm diameter silica fibers, 0.06 mol $AgNO_3$, heated for 60 min) was seen to increase with increase in temperature from 400 to 600 °C. Further increase in temperature of the fibers to 800 °C did not cause any sharp increase in the size of the silver nanoparticles. Similarly, when the time for which the fibers were heated (Figure 2A,D, 250 nm diameter silica fibers, 0.06 mol $AgNO_3$, heated at 400 °C) was increased from 60 to 150 min, an increase in the size of the silver nanoparticles was noticed. This effect of temperature and time on the size of the silver nanoparticles can be explained by a thermal sintering

(54) Flynn, J. H. *Handb. Therm. Anal. Calorim.* **2002**, *3*, 587−651.

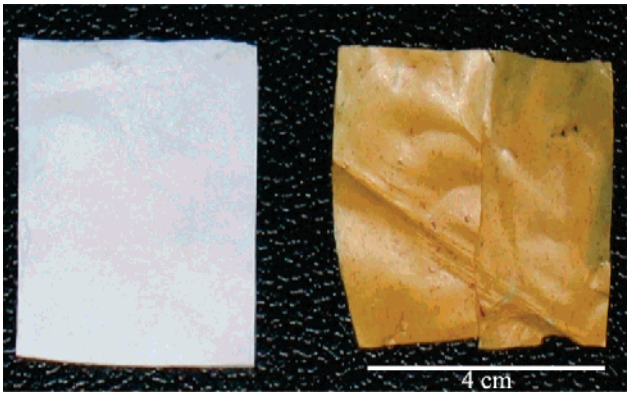

Figure 5. (A) White electrospun PMCM modified silica fiber mats containing silver nitrate ($AgNO_3$) before heat treatment. (B) Golden yellow porous silica fiber mats containing 10 wt % silver nanoparticles after heat treatment at 600 °C for 60 min. Scale bar: 4 cm.

process.[55,56] Thus, the silver ions present in the silica fibers flock together and form a cluster of ions that form nanoparticles. With increase in temperature, coalescence of nanoparticles takes place, leading to an increase in the size of the silver nanoparticles. These nanoparticles keep growing in size with increase in temperature, finally reaching a maximum size limit, due to the interference of the rigid silica walls of the porous fibers, which prevent the merging of individual nanoparticles with their neighbor.[55] Figure 2A,E shows TEM micrographs of heat-treated (250 nm diameter silica fibers, heated at 400 °C for 60 min) silica fibers, electrospun using 0.06 and 0.1 mol $AgNO_3$, respectively. The increase in concentration of $AgNO_3$ from 0.06 to 0.1 mol leads to an increase in number and size of silver nanoparticles.[27] Similarly, with the increase in diameter of silica fibers from 100 to 250 nm, the average size of the silver nanoparticles also increases (Figure 2F, 0.06 mol $AgNO_3$, heated at 600 °C for 150 min). Although this is not fully understood, we suggest that, with the increase in the fiber diameter, the PMCM copolymer in the fibers during electrospinning might be less uniformly dispersed, which leads to the formation of larger pores during thermal treatment. The large pores thus formed are then occupied by the larger silver nanoparticles.

The optical properties of heat-treated silica fibers were studied to further evaluate the distribution and size of silver nanoparticles in the fibers. Before heat treatment, the PMCM modified silica fiber mats containing 0.06 mol $AgNO_3$ are white in color. Upon heating, these fiber mats change to a light golden yellow color as seen in Figure 5, owing to the surface plasma resonance (SPR) of the silver nanoparticles produced in the silica fibers during heat treatment. SPR is a characteristic feature of metal nanoparticles between the sizes of 2 and 50 nm.[22,46] Here the electrons freely oscillate on the metal particle surface and adsorb electromagnetic radiation from particular energy levels. Particles less than 2 nm, on the other hand, do not show this phenomenon due to the presence of electrons in discrete energy levels.[22,46] Figure 6A shows UV spectra of heat-treated silica fibers, which

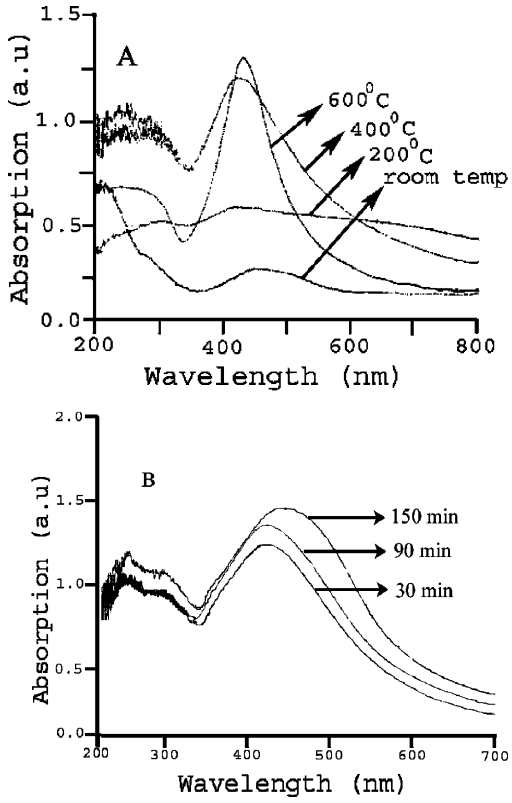

Figure 6. Optical spectra of porous silica nanofibers containing 10 wt % silver nanoparticles: (A) heat treated at different temperatures for 30 min and (B) heat treated for various periods of time at 400 °C.

exhibit well-defined plasmon peaks with narrow size distribution of silver nanoparticles. The fibers heated up to 200 °C for 30 min do not show any plasmon peaks due to the incomplete formation of silver nanoparticles in the sample. On the other hand, samples heated up to 400 and 600 °C for 30 min show sharp spectral bands for silver at around 406 and 410 nm, respectively. The shift in wavelength, seen in fibers at higher temperature, is due to the increase in size of silver nanoparticles. Similarly, Figure 6B shows UV spectra of fiber samples heated to 400 °C for 30, 90, and 150 min. As the time of heat treatment is increased, the plasmon peak shifts to higher wavelength, due to the increase in size of the silver nanoparticles.[22,26,57] Figure 7 shows XRD spectra for silica fibers heat treated to various temperatures and time. The diffused reflection peaks at 2θ value of 20° observed in all the samples are indicative of the amorphous nature of sol−gel silica materials.[58] The peaks at 2θ values of 38.2°, 44.5°, 64.6°, and 77.5° correspond to the (111), (200), (220), and (311) crystal planes of silver particles.[59] The calculated *d*-spacing (Table 2) of the silver particles was found to be consistent with the International Centre for Diffraction Data (Table 2) obtained from JCPDS files (no. 41-1402), indicating that the silver nanoparticles have cubic symmetry. Apart from measurement of the size of silver nanoparticles via TEM micrographs, the average size of the silver nanoparticles (Table 1) was also calculated using Bragg's and Sherrer's

(55) Moon, K. S.; Dong, H.; Maric, R.; Pothukuchi, S.; Hunt, A.; Li, Y.; Wong, C. P. *J. Electronic Mater.* **2005**, *34* (2), 168−175.
(56) Buffat, P. A. *Phil. Trans. R. Soc. London, Ser. A* **2003**, *361* (1803), 291−295.
(57) Ritzer, B.; Villegas, M. A.; Fernandez Navarro, J. M. *J. Sol-Gel Sci. Technol.* **1997**, *8* (1/2/3), 917−921.
(58) Choi, S. S.; Lee, S. G.; Im, S. S.; Kim, S. H.; Joo, Y. L. *J. Mater. Sci. Lett.* **2003**, *22* (12), 891−893.
(59) Mitrikas, G.; Trapalis, C. C.; Kordas, G. *J. Non-Cryst. Solids* **2001**, *286* (1,2), 41−50.

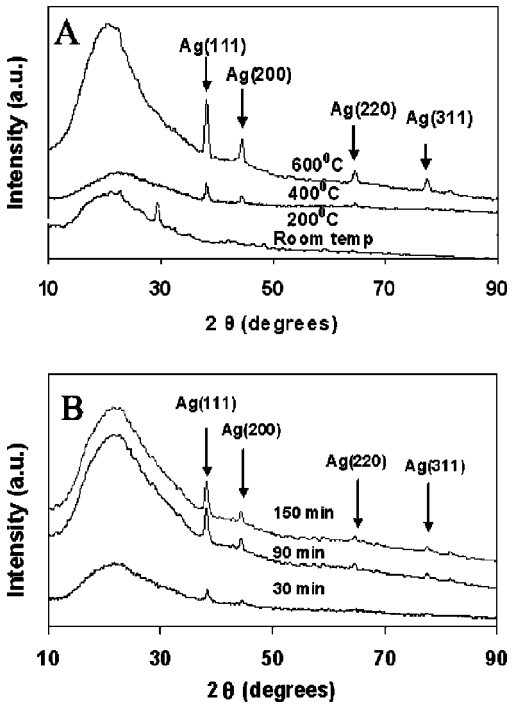

Figure 7. X-ray diffraction patterns for silica fibers containing 10 wt % silver nanoparticles: (A) heat treated at various temperatures for 30 min and (B) heat treated for various periods of time at 400 °C.

Table 2. Comparison of Calculated *d*-Spacing (d_{hkl}) Values of Silver Nanoparticles with Data from the International Centre for Diffraction Data Obtained for Silver from JCPDS Files (No. 41-1402)

$(hkl)^a$	calcd $d_{hkl}{}^b$	d_{hkl} from JCPDS files[c]
(111)	0.2356	0.2359
(200)	0.2036	0.2043
(220)	0.1444	0.1445
(311)	0.1231	0.1231

[a] Cubic crystal lattice planes of silver nanoparticles. [b] Calculated *d*-spacing (inter planar spacing in Å) of silver particles ($\lambda = 2d \sin\theta$) present inside silica fibers. [c] International Centre for Diffraction Data obtained for silver from JCPDS files (no. 41-1402).

equation ($D = 0.9\lambda/\text{fwhm} \cos\theta$, D is the average particle size in Å, fwhm is the full width of the peak at half-maximum, and θ the diffraction angle).[21] In all, samples heated to 300 °C did not show any peaks for silver, indicating that the silver ions were not yet converted to silver nanoparticles. As the samples were heated to higher temperature and for longer time, the peaks for silver crystals appeared and also increased in intensity.

Silver nanoparticles have been studied as a catalyst in reduction reactions of nitrophenols, nitroanilines, and various dyes like methylene blue (MB), fluorescein (F), and so forth.[23−25] Reduction of MB by $NaBH_4$ is used as a standard for determining the catalytic activity of the silver nanoparticles encapsulated in the porous silica fibers. In agreement with previous results, the reduction of MB, if it occurs at all, is insignificant in the absence of silver particles.[23,60,61] However, in the solution containing silver particles, the reduction of the dyes by $NaBH_4$ is completed within 2−20 min. Choice of MB dye for testing the catalytic activity of

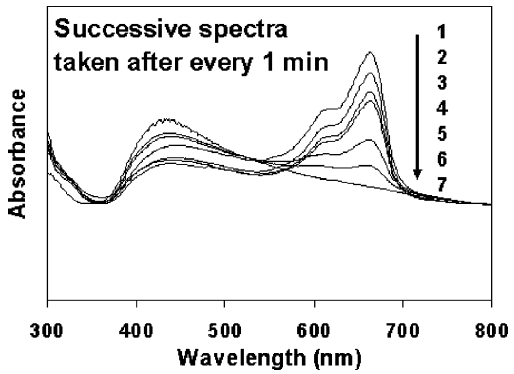

Figure 8. Successive UV−vis spectra (taken every 1 min) of methylene blue (MB) dye reduction, using silica nanofibers containing silver nanoparticles as the catalyst and $NaBH_4$ as the reducing agent.

the PSFSP is based on two factors: (1) the dye changes from blue to colorless when reduced, thus giving a sharp visible color change, and (2) the absorbance maximum (λ_{max}) for MB is around 665 nm which does not interfere with the λ_{max} of silver nanoparticles which is around 420 nm.[46]

The preliminary catalytic testing for PSFSP was carried out by reduction of 2 mL of MB (0.01 mol/L) in water using 0.10 g silica fibers containing approximately 10 wt % silver nanoparticles as catalyst and 1 mL of $NaBH_4$ (0.1 mol/L) as the reducing agent. The progression of the catalytic reduction of MB can be easily followed (Figure 8) by the change in optical density at the λ_{max} of 665 nm (oxidized form of MB). Evidently, the absorbance at λ_{max} of MB gradually decreases with the reaction time, which is indicative of the reduction of MB from blue to colorless. As expected, the catalytic reduction of MB proceeded successfully, and no deactivation or poisoning of the catalyst was observed. The band at 420 nm (which comes from the silver nanoparticles present inside the fibers) was not very prominent at the initial stages of the reaction, but as the reduction of MB proceeded, the band at 665 nm (oxidized form of MB) disappeared and the band at 410 nm (silver nanoparticles present inside the fibers) became prominent. The induction period of 1 min seen at the initial stage of the reaction could be due to the time required for the dye to enter the porous network of the silica fibers and come in direct contact with the silver nanoparticles. The entire reduction reaction experiment was conducted under nitrogen because oxygen might interfere with the reduction of MB.[61] A blank test containing a mixture of MB dye plus $NaBH_4$ reducing agent, with pure silica fibers containing no silver particles, did not show any reduction or color change for more than 24 h. Currently, we are carrying out systematic experiments to measure quantitatively the number and amount of silver nanoparticles in the fibers that are accessible for catalytic reactions.

Conclusion

In this study, novel catalytic silica nanofibers containing silver nanoparticles have been successfully synthesized via a new, simple method consisting of electrospinning of a sol containing TEOS, trialkoxysilyl functionalized polymethacrylate PMCM, and silver nitrate, followed by thermal treatment to remove polymethacrylate by pyrolysis and to convert silver nitrate to silver nanoparticles. The density and size of the

(60) Pal, T.; Sau, T. K.; Jana, N. R. *J. Colloid Interface Sci.* **1998**, *202* (1), 30−36.
(61) Pal, T.; Sau, T. K.; Jana, N. R. *Langmuir* **1997**, *13* (6), 1481−1485.

silver nanoparticles present in fibers can be readily controlled, by varying the diameter of the electrospun fibers, concentration of silver nitrate salt and the polymethacrylate precusor, and thermal treatment conditions. The silver nanoparticles in the silica fibers exhibit good catalytic properties based on the results from the silver-catalyzed reduction of MB dye with sodium boron hydride as reducing agent.

Acknowledgment. This work was supported in part by the National Institutes of Health (Grant DE09848), by the National Natural Science Foundation of China via a major International Cooperative Research Grant to the Jilin University Alan G. MacDiarmid Institute, and by the Nanotechnology Institute of Southeastern Pennsylvania.

Supporting Information Available: Schemes for chemical changes of silica fibers during heat treatment, elemental analysis and X-ray mapping of fiber samples, experimental and calculated wt % of silica present in the heat-treated fibers. This material is available free of charge via the Internet at http://pubs.acs.org.

CM061331Z